

Eng. Research Bull.  
Faculty of Eng. & Tech.  
Menoufia University  
Vol.VII Part2, 1985.

PP. 17-40

A MODEL FOR PITTING PRODUCED BY CAVITATION

Sobeih M.A.Selim\*

ABSTRACT

The present paper is concerned with the mechanism of cavitation erosion. A theoretical model for the formation of a single pit produced by a shock wave radiated from the collapse centre of a cavitation bubble is presented and the model developed to give the average surface slope of the eroded surface. This model includes many parameters controlling the cavitation damage such as the cavitation number, flow velocity, inception cavitation number and material properties. The model predicts a critical velocity below which no pitting can occur. Preliminary erosion experiments were conducted in water tunnel using pure aluminium specimens subjected to cavitating flow produced by a circular cylinder. The surface deformation produced on specimens was analysed by a surface finish measuring device. From the surface profiles, the surface slope and pit radius were computed. The results were compared with the theoretical model and a good agreement was found. This agreement means that the roles played by cavitation number and velocity are consistent with the present model.

---

\* Lecturer, Department of Mechanical Power Engineering,  
Faculty of Engineering and Technology, Menoufia  
University.

## INTRODUCTION

Many investigations agree that cavitation erosion is the result of totally mechanical attack [1,2,3]. The mechanical cavitation damage is due to the highly transient imposition of very intense and highly local forces on the surface. It is expected that there will be two types of damage produced by a cavitation bubble collapse; one is the effect of the shock wave radiated from the collapse centre and the other is the microjet formed when the bubble collapses near a solid surface. Such a microjet is generated when the bubble collapse becomes substantially nonsymmetrically. The materials subject to the impact of the shock wave or microjet undergo plastic deformation and become workhardened. Many investigators showed that the damage was due to plastic deformation caused by the impact of microjets developed by the collapse of bubbles near to a solid surface [1,4,5]. This theory is in contrast to the shock wave pressure theory of Rayleigh [6]. Preece et al. [3] stated that the surface deformation of face centred cubic metals in a vibratory system is by shock waves and that the material removal is by ductile rupture from the lips of the craters. Shima [7] and Yoshiyaki [8] reported that the damage was due to shock waves, microjets or both depending on the distance of the solid surface from the collapse centres. Rao et al., [9] and Eisenberg et al., [10] also are of the view that the damage may be due to either shock waves or microjets caused by the collapse of bubbles near solid surfaces. Knapp [11] and Thiruvengadam [12] support the shock wave mechanism concept.

In order to quantify the damage produced it is usual to postulate that a part of the energy stored by the cavitation bubble appears as energy dissipated in plastic work. Attempts have been made on this basis to correlate

flow conditions and erosion rate [13,14,15]. Generally, all these attempts suffer from the fundamental weakness that it is very difficult to estimate accurately the amount of energy from cavitation bubble which lost by reflection from the surface and rebound of the collapse bubble, i.e, the energy which never reaches the surface.

Therefore, the intent of this work is to establish a simple model for the formation of a single cavitation pit produced by a shock wave radiated from the centre of collapse. This model based on the idea of momentum transfer from the shock wave to the damaged surface.

### THEORETICAL CONSIDERATIONS

The general kinematic features of a shock wave collision on a smooth, plane surface will be described on the basis of current analysis and experimental observations.

When ductile materials are subjected to impact by a shock wave the deformation can be categorized as follows: 1. Elastic 2. Elastic plus plastic 3. Hydrodynamic, i.e., viscous. For elastic deformation (category 1) there is no apparent damage after impact, whereas for category 2 a permanent deformation occurs. In category 3 the combination of materials properties and impact conditions is such that the solid responds as a viscous fluid. This occurs primarily in "hypersonic impacts" such as for example, collisions between meteoroids and spacecraft. This type of collision is not concern for most other types of engineering applications.

Characteristic stages for the impact of a shock wave of speed  $v_s$  with a plane rigid surface at rest are shown in Figure 1. The overall impact sequence can be divided into

two phases: the pressure build-up phase and the pressure release phase. The solid surface is at rest, its initial velocity is zero; and the impact velocity of the shock wave is its initial velocity  $v_s$ . It is assumed for simplicity that the pressure behind the shock wave,  $P_s$ , is linearly related to the acoustic particle velocity,  $V_s$ , i.e.,  $P_s = \rho_0 C_0 V_s$ . Upon contact the wave will be reflected from the surface and the pressure will rise to  $P$  and the particle velocity will fall to  $u$ . The discontinuity in the velocity at initial contact is thus  $u$  for the solid surface and  $(V_s - u)$  for the shock wave. On applying the principle of conservation of momentum across the resultant pressure rise is given by

$$\Delta P = \rho C \Delta u \quad (1)$$

where  $C$  and  $\rho$  are respectively the speed of sound and density of the liquid,  $\Delta u$  is the discontinuity in the shock wave velocity and equals to  $(v_s - u)$ ,  $\Delta P$  is the resultant pressure rise and equals to  $(P - P_s)$ . Substituting the values of  $P = P - P_s$ ,  $P_s = \rho C V_s$  and  $u = V_s - u$  in equation (1), the velocity of deformation ( $u$ ) is given by the following expression,

$$u = 2 V_s - P / \rho C \quad (2)$$

It is postulated that the indentation pressure remains constant at the value necessary to produce the plastic flow which equals the yield stress ( $Y$ ) of the solid. Therefore, on rearranging equation (2) to give the velocity of deformation as follows

$$\begin{aligned} u &= 2 V_s - Y / \rho C \\ &= 2 V_s - u_0 \end{aligned} \quad (3)$$

where  $Y / \rho C = u_0$  is the critical shock wave impact velocity.

For impact velocities less than  $u_0$ , it would be expected that shock wave impact would cause purely elastic strain in the solid. However, at impact velocities higher than  $u_0$  plastic deformation of the solid occurs. In other words the deformation can only occur when  $V_s > \frac{1}{2} u_0$  or when  $P_s > \frac{1}{2} Y$ .

After initial contact the shock wave has indented the solid surface to a depth  $X$ . The depth at the centre of the pit can be found from the product of deformation velocity and time available for deformation, in equation form,

$$X = u \cdot \tau \quad (4)$$

If the small delay caused by the propagation of a release wave in the solid is neglected, the time available for deformation ( $\tau$ ) will consist of the time for the wave to spread from the centre of impact to the point where deformation ceases plus the time for the release wave in the liquid to travel from the edge to the centre. Thus the time available for deformation,  $\tau$ , is given by,

$$\tau = \frac{r-L}{c} + \frac{a}{c} \quad (5)$$

From figure (1) it can be seen that  $r$  is given by,

$$r = \sqrt{L^2 + a^2} \quad (6)$$

substituting equation (6) into (5), the available time for deformation is given by,

$$= \frac{L}{c} \left[ \sqrt{\left(\frac{a}{L}\right)^2 + 1} + \frac{a}{L} - 1 \right] \quad (7)$$

Substituting equations (3) and (7) into (4) the depth ( $x$ ) is obtained by

$$X = (2V_s - u_0) \frac{L}{c} \left[ \sqrt{\left(\frac{a}{L}\right)^2 + 1} + \frac{a}{L} - 1 \right] \quad (8)$$

Assuming that the shock wave is attenuated as  $1/r$  where  $r$  is the distance from the collapse centre, then the edge of the deformation region may be defined by the circle when the plastic flow ceases and the shock strength has fallen to  $\frac{1}{2} Y$ . If the collapse centre is a distance  $L$  from the surface and  $P_s$  is the shock strength at the surface, then the product  $P_s \cdot L$  represents the effective source strength. If the radius of the deformation region is "a" then

$$P_s \cdot L = \frac{1}{2} Y \cdot \sqrt{L^2 + a^2}$$

and hence the radius "a" is given by

$$a = L \sqrt{\left(\frac{2 P_s}{Y}\right)^2 - 1} \quad (9)$$

Hence the average surface slope, i.e.,  $\frac{x}{a}$  of the resulting pit can be found by combining (8) and (9) i.e.

$$\frac{x}{a} = \frac{1}{c} \left(2V_s - \frac{Y}{f c}\right) \left[ \frac{\left(\frac{2V_s}{u_o}\right) - 1}{\sqrt{\left(\frac{2V_s}{u_o}\right)^2 - 1}} + 1 \right] \quad (10)$$

Assuming that the impact velocity of the shock wave is proportional to the bubble wall velocity ( $R^\circ$ ), i.e.,  $v_s \sim R^\circ$ . Rayleigh's [6] theoretical studies have indicated that the magnitude of the bubble wall velocity ( $R^\circ$ ) and the pressure difference ( $\Delta P_b$ ) causing the collapse of the cavitation bubble are related by,

$$R^\circ \sim \sqrt{\frac{\Delta P_b}{f}} \quad (11)$$

where  $\Delta P_b$  is the difference between the pressure outside the bubble and inside the bubble at the beginning of the collapse. According to reference [16] the pressure difference  $\Delta P_b$  is given by

$$\Delta P_b \sim \rho U^2 (1 + \sigma) (1 + \sigma_i) \quad (12)$$

where  $U$  and  $\sigma$  are fluid velocity and the cavitation number at the throat of the cavitating body,  $\sigma_i$  is the inception cavitation number at the throat of the cavitating body. Hence, substituting equation (12) into (11) and using the assumption that  $V_s \sim R^0$ , the impact velocity of the shock wave ( $V_s$ ) is given by

$$V_s = k U (1 + \sigma)^{\frac{1}{2}} (1 + \sigma_i)^{\frac{1}{2}} \quad (13)$$

where  $k$  is constant. Similarly it is assumed that the critical velocity to produce plastic work ( $u_o = Y/\rho C$ ) is given by the following expression

$$u_o = k U_o (1 + \sigma)^{\frac{1}{2}} (1 + \sigma_i)^{\frac{1}{2}} \quad (14)$$

Combining equation (10), (13) and (14), the average surface slope ( $\frac{x}{a}$ ) of the resulting pit in terms of the flow condition is given by

$$\frac{x}{a} = k_1 (1 + \sigma)^{\frac{1}{2}} (1 + \sigma_i)^{\frac{1}{2}} \left( U - \frac{U_o}{2} \right) \left[ \frac{2U - U_o}{\sqrt{4U^2 - U_o^2}} + 1 \right] \quad (15)$$

where  $k_1 = 2k/C$  and  $U_o$  is the critical flow velocity to produce pit.  $k_1$  and  $U_o$  can be estimated from relevant test results.

#### EXPERIMENTAL APPARATUS

Preliminary erosion tests were conducted in a cavitation research water tunnel with a parallel sided working section of 40 x 20 mm cross section at the Faculty of Engineering and Technology, Menoufia University. Details of the design and description of this tunnel can be found in El-Danaf [17]. The tunnel was designed so that the flow rate and pressure

in the working section could be varied independently. The flow rate through the test section could be controlled by a by pass valve and the pressure by a control valve connected to an external compressed air supply. The cavitation was produced by a 25 mm diameter cylindrical body fitted centrally into the working section of the cavitation tunnel as shown in Figure (2). The erosion was determined using a plate of material of size 40 x 140 mm and 6 mm thick mounted on a side wall of the working section. The material used was pure Aluminium and this is was chosen because it exhibits almost perfect plasticity and is very easily eroded. The specimens were prepared by polishing to give a fine finish on the whole surface of the specimen.

For the first series of the cavitation tests, the tunnel was run at a constant cavitation number ,  $\sigma$ , appropriate to conditions in the throat and defined by

$$\sigma = \frac{P - P_v}{\frac{1}{2} \rho U^2}$$

where P and U are respectively the pressure and velocity in the throat. The value of  $\sigma$  chosen was 0.06 corresponding approximately to the maximum noise radiated from the collapse of the bubbles, and the throat velocity was varied over the range 19 to 30 m/s. The second series of tests consisted of running the tunnel at a constant velocity of 26 m/s and varying the cavitation number over the range 0.025 to 0.09.

The expected error in the cavitation number is about + 6% . While the possible error in the flow velocity is about + 1 %.

#### MEASUREMENT OF SURFACE DEFORMATION

The eroded specimens were analysed using a FÖRSTER Profilograph Model 5815 at the Faculty of Engineering and Technology, Helwan University. The surface profiles were used to find the surface slope and the average pit radius. The scanning device used to measure the surface roughness



has a diamond stylus with a rounded tip about 10  $\mu\text{m}$ . The stylus speed and the operative length of traverse were kept the same for all the tests. This was accomplished by setting the speed of the stylus across the specimen surface equal to 0.5 m/s and the operative length of traverse equal to 8 mm.

The surface slope was obtained from the surface profiles. It was estimated by summing the modulus of the lateral movement of the stylus and dividing by the length of the trace. On assuming that the average pit depth was twice the centreline average depth, the average pit radius was deduced by dividing the average pit depth by the previously calculated average surface slope. Further details of the method used to analyse the surface profiles are given in appendix 1. The expected error in the surface slope is approximately  $\pm 8\%$  and in the average pit radius is about  $\pm 6\%$ .

Photographs of some erosion specimens were taken using optical metallurgical microscope which is provided with a camera.

#### EXPERIMENTAL RESULTS AND DISCUSSION

Typical figures (3) to (6) show the effect of exposure time on the surface roughness for the 25mm circular cylinder with sidewall specimens. Figures (3) and (4) are for tests conducted at a constant cavitation number of 0.06 and various flow velocities of 30m/s and 19 m/s. While figures (5) and (6) are for tests conducted at a constant flow velocity of 26 m/s and different cavitation numbers of 0.09 and 0.025. Generally, these figure indicate that the surface roughness and the number of pits increase with time.

From the surface profiles determined by FÖRSTER Profilograph, the surface slope and the pit radius were

calculated and plotted as function of exposure time. Figure (7) shows the variation of surface slope with exposure time at various flow velocities ranged from 19 m/s to 30 m/s with a constant cavitation number of 0.06. In general Figure (7) indicates that the surface slope increases with time. It appears that the surface slope varies linearly with exposure time, the best fit straight lines to the data can be calculated using least squares are shown in Figure (7). It is reasonable to assume that the intercept of the straight line at zero time on the surface slope axis gives the level established very soon after the start of exposure, since the impact time is very small.

The variation of the surface slope at zero time with flow velocity at constant cavitation number is shown in Figure (8). Also this figure shows equation (15) applied to the experiments at a constant cavitation number of 0.06 with varying flow velocity. As shown in Figure (8) a good correlation is in fact found between the measured and the calculated surface slope using equation (15). The constants  $k_1$  and  $U_0$  in equation (15) were computed using the measured surface slope at 30 m/s and 23 m/s. These constants are  $k_1 = 1.53 \times 10^{-3}$  s/m and  $U_0 = 13.6$  m/s. It is clear that the threshold velocity below which no pitting on Aluminium can occur is 13.6 m/s.

Figure (9) shows the variation of the average pit radius with exposure time at various flow velocities. This figure indicates that the average pit radius may be independent of exposure time. Therefore, the mean values were determined and plotted as a function of flow velocity at constant cavitation number as shown in Figure (10). Figure (10) indicates that the mean value of pit radius varies with flow velocity, showing a slight increase with

flow velocity. A best fit line using least squares indicates that the slope is very small.

Figure (11) shows the variation of the surface slope with exposure time at various cavitation number numbers with constant flow velocity of 26 m/s. This figure shows a similar trend to that shown in Figure (7). The values of surface slope at zero time found by using the method of least squares as a function of cavitation number are shown in Figure (12). Figure (12) shows that the surface slope at zero time varies with cavitation number, showing an increase with increasing the cavitation number. Also Figure (12) shows the equation (15) applied to the experiments at a constant flow velocity of 26 m/s with varying cavitation number. A good correlation is in fact found between the measured and calculated surface slope using equation (15). This agreement means that the roles played by cavitation number is consistent with the present analysis.

Figure (13) shows the variation of average pit radius with exposure time at various cavitation numbers and constant flow velocity of 26 m/s. This figure shows considerable scatter in the data indicating that the average pit radius is probably independent of time. Figure (14) is a plot of mean pit radius versus cavitation number. As shown in Figure (14), there is clearly a decrease in the mean pit radius with increasing cavitation number. The reason for this is that as the cavitation number increases the maximum bubble size decreases and therefore it appears that the mean value of pit radius may be proportional to the maximum bubble size. If it is assumed that the relationship between the mean pit radius and cavitation number is a power law, it can be shown by the method of least squares that the index which gives the best fit is - 0.32 (i.e.  $a \sim \sigma^{-0.31}$ ).

### CONCLUSIONS

1) A simple theoretical model has been developed to describe the formation of single pit produced by a shock wave from cavitation. The basic accomplishment of this initial effort has been to be able determine the surface slope of the cavitation number, flow velocity, inception cavitation number and material properties. This effort will provide a firm foundation for the development of more complete model of the erosion mechanism in which the rate of weight loss can be predicted.

2) A critical flow velocity of 13.6 m/s below which not pit occur on pure Aluminium surface gives the best agreement with experiments.

3) The results indicates that the surface slope is dependent on the flow velocity and cavitation number as expected from the theoretical model. The pit radius is found to increase slightly with velocity but varies inversely as cavitation number.

4) A good agreement between the experiments results and theoretical analysis was observed.

### REFERENCES

- [1] Hammitt, F.G.,; "Collapse Bubble Damage to Solids," Cavitation state of knowledge, Ed. by Robertson, J. and Wislicenus, G.F., ASME, New York, NY, 1969.
- [2] Hammitt, F.G.: "Cavitation and Multiphase Flow Phenomena", McGraw Hill, Int. Book Co., New Yorks, 1980.
- [3] Vyas, B. and Preece, C.M.: "Cavitation of F.C.C. Metals", Metall Trans., Vol.8A, Jan., 1977.

- [4] Robinson, M.J. and Hammitt, F.G1,: "Detailed Damage Characteristics in a Cavitating Venturi", Trans ASME, Jr of Basic Engr., No.7 Ser.D, Vol.89, March 1967.
  
- [5] Brunton, J.H., Rochester, M.C.,:"Erosion of Solid Surfaces by the Impact of Liquid Drops", in Erosion, Ed., by C.M.Preece, Vol,16, Academic Press, New York. 1979.
  
- [6] Rayleigh, Lord,"On the Pressure Developed in a Liquid During the Collapse of a Spherical Cavity", Phil.Mag., 1917,34, 94.
  
- [7] Shima et al. ,: "Mechanism of Impact Pressure Generation from Spark - Generated Bubble Collapse Near a wall", AIAA Jr., Vol.21, No.1, Jan.1983.
  
- [8] Yoshiyaki Tsude et al.,:"Experimental studies of shock Generation at the Collapse of Cavitation Bubble", Bulletin JSME, Vol.25, No.210, Dec.1982.
  
- [9] Lakshmana Rao et al.,:"Prediction of Cavitation Erosion and the Role of Material Properties",Jr. Inst.Eng.(India) Civil Eng.Div., V58, Sep./Nov. 1977.
  
- [10]Eisenberg, P.et al.,:"Cavitation and Impact Erosion Concepts", ASTM, STP 474, 1970.
  
- [11] Knapp, R.T.,:"Recent Investigations of Cavitation and Cavitation Damage", Trans.ASME, Vol.77,1955.
  
- [12] Thiruvengadam, A.,:"Theory of Erosion", Hydronautics Inc.Tech.Rept., March,1967.

- [13] Klastrup Kristensen, J. et al.,: "A Simple Model for Cavitation Erosion of Metals", Jr. Phys. D. Appl. Phys., Vol. 11, 1978.
- [14] Kato, H.,: "On the Prediction Method of Cavitation Erosion From Model Test", IAHR Symposium on Two phase Flow and Cavitation in Power Generation Systems, Grenoble, March 1976.
- [15] Raabe, J.: "Theoretical Approach of Erosion Rate Versus Speed and Cavity size on Wall-attached Cavitation", ASME Symposium on Cavitation Erosion in Fluid Systems, Boulder, Colorado, June 1981.
- [16] Selim, S.M.: "A Theoretical Study on Cavitation Erosion Rate", ASME symposium on Cavitation in Hydraulic Structures and Turbomachinery, FED-Vol. 25, Albuquerque, New Mexico, June, 1985.
- [17] El-Danaf, R.A.: "Study of Cavitation Inception in Fluid Flow", M.Sc. Thesis, Mech. Power Eng. Dept., Menoufia University, July 1985.

#### APPENDIX 1

##### Analysis of Surface Profiles

The erosion specimens were analysed using a FORSTER Profilograph Model 5815 to give the centerline average depth directly and to produce surface profiles, which were then used to find the average modulus surface slope ( $\frac{x}{a}$ ). This is defined by

$$\frac{x}{a} = \frac{\sum |\Delta Y|}{l}$$

where  $\Delta Y$  is the ordinate difference between adjacent

turning points and  $\ell$  is the length of the sample. This definition can be expanded for ease of computation to give,

$$\frac{x}{a} = \frac{2}{\ell} \left[ \frac{Y_1}{2} - Y_2 + Y_3 - Y_4 + \dots + \frac{Y_n}{2} \right]$$

Where the signs alternate regardless of the number of turning points considered (See Fig. A).

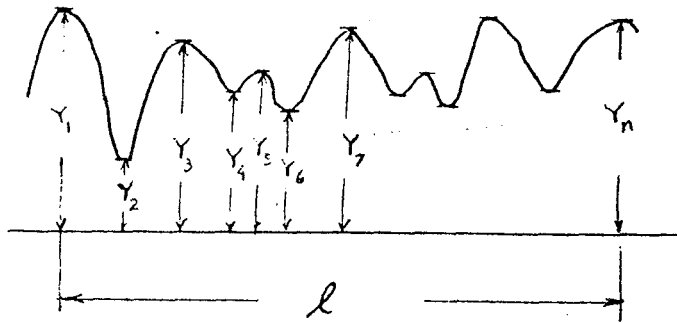


Fig.A. Definition Sketch for average surface slope.

#### Average Pit Radius

This can be defined as

$$a = \ell / (n-1)$$

where  $n$  is the number of  $Y$  co-ordinates considered. It can be also calculated from average slope and average depth of pit as follows

$$\text{Average radius} = \frac{\text{Average Depth}}{\text{Average slope}}$$

The average depth can be obtained from the following expression,

$$\text{Average Depth} = \frac{\sum |\Delta y|}{n - 1}$$

The values of the average pit depth correlate well with the centre line average recorded by the FÖRSTER Profilograph, being approximately equal to two times the centre line average. Therefore, the average pit radius can be alternatively defined in terms of the centre line average (CLA) as follows,

$$\text{Average radius} = \frac{2 \times \text{CLA}}{\text{Average Slope}}$$

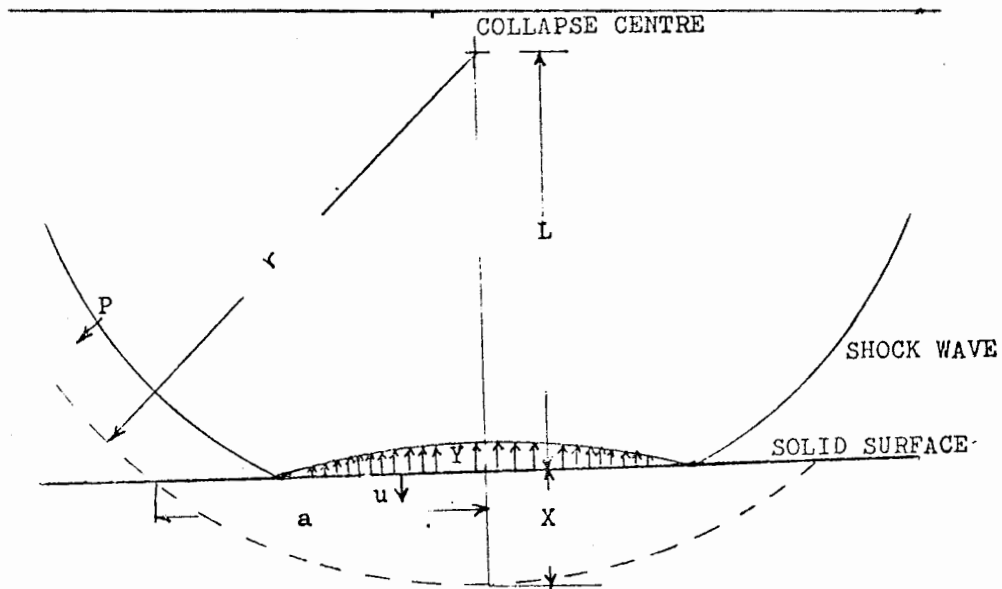


Fig 1 :Sketch of contact geometry between shock wave and a solid surface.

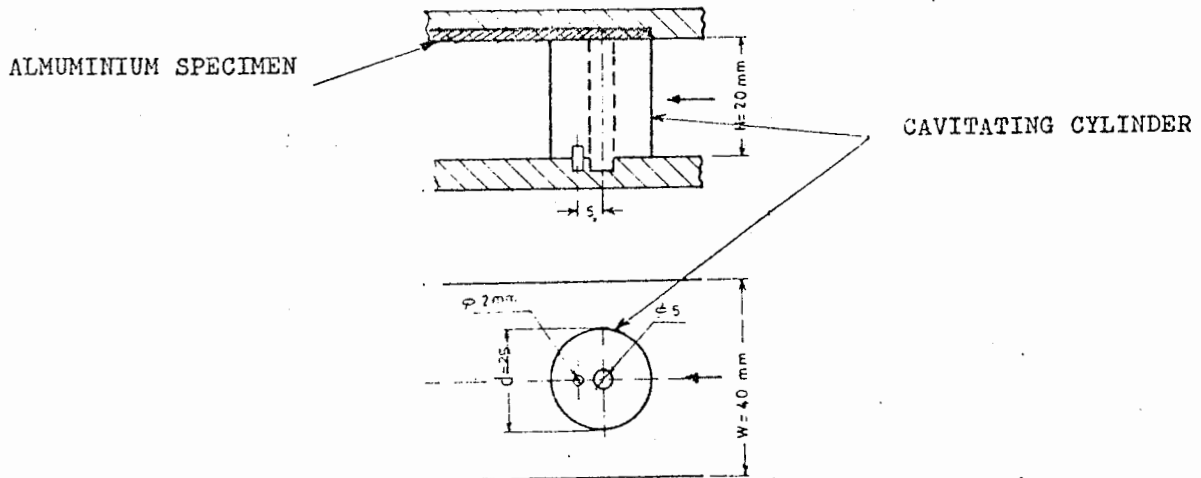


Fig 2 Position of cylinder and specimen in the test section of the Water Tunnel.



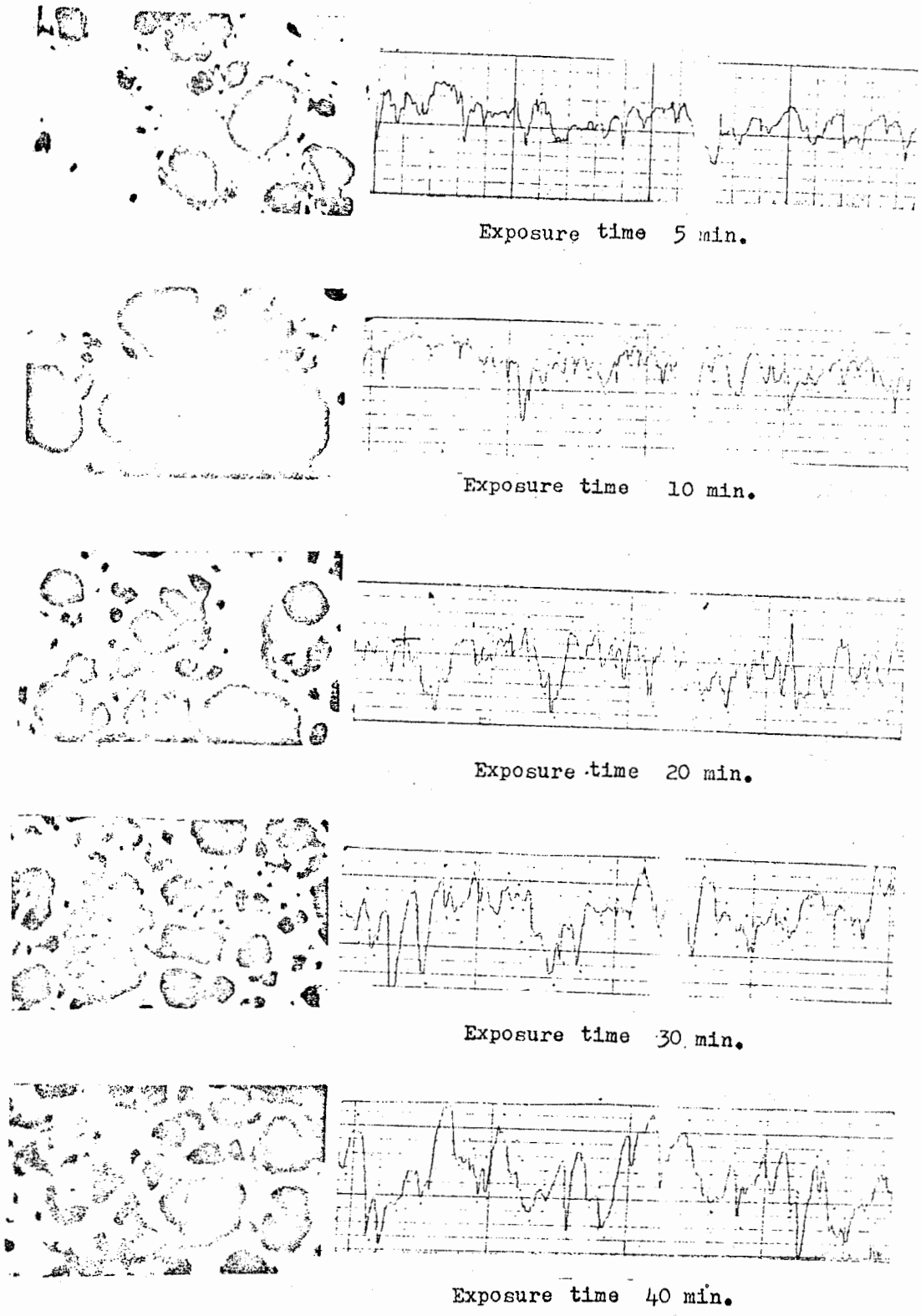
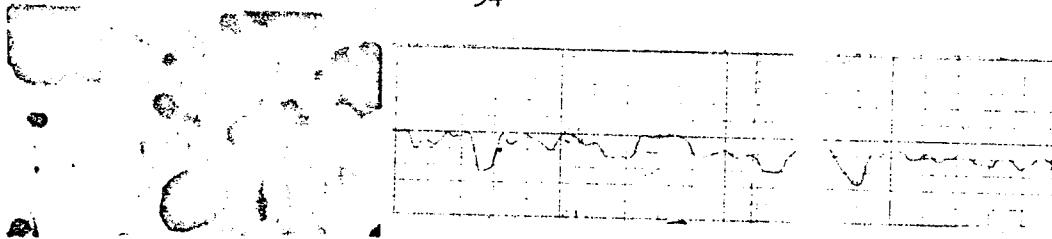
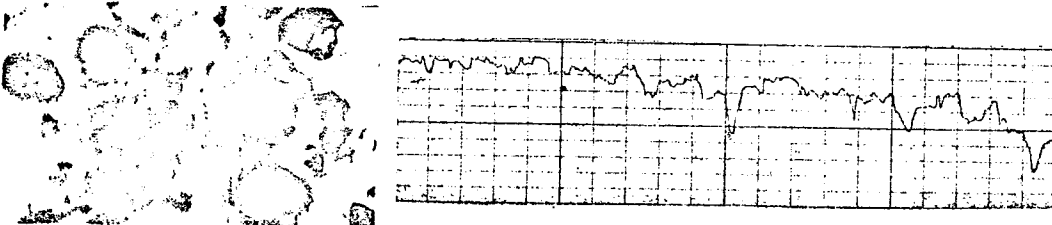


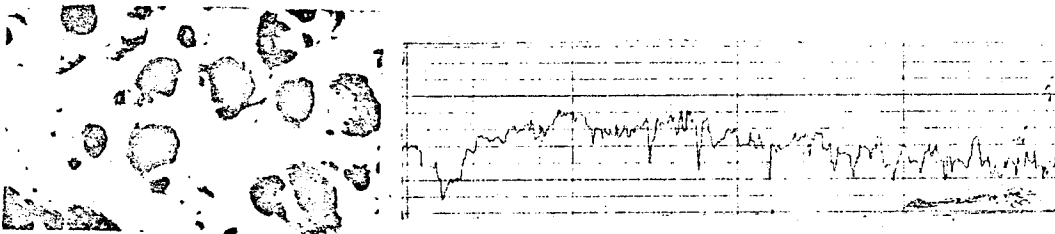
Fig 3 Photographs and profiles of typical damaged specimens at various exposure times,  $U = 30$  m/s and  $\sigma = .06$ .



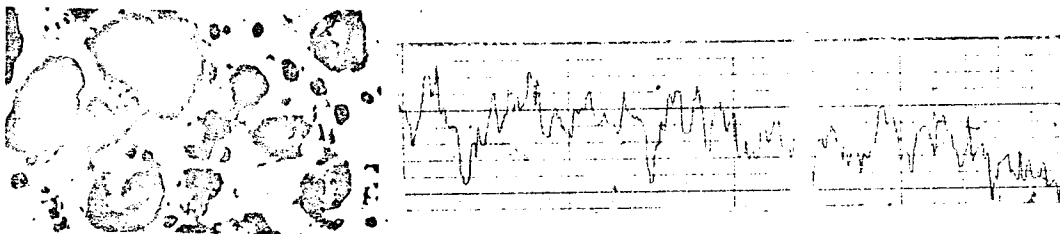
Exposure time 30 min.



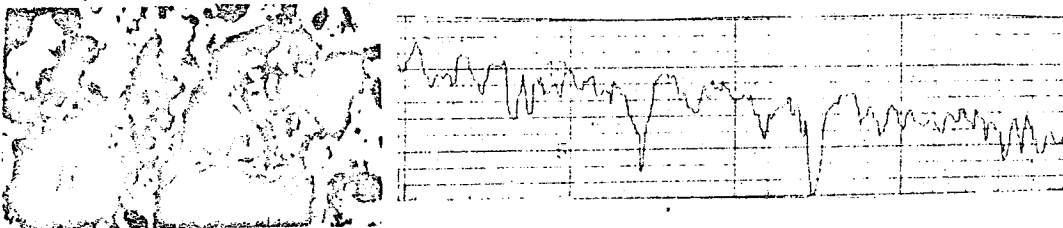
Exposure time 90 min.



Exposure time 140 min.

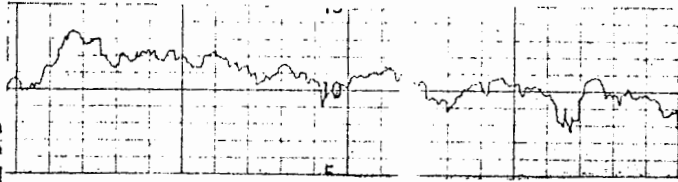


Exposure time 3 hrs

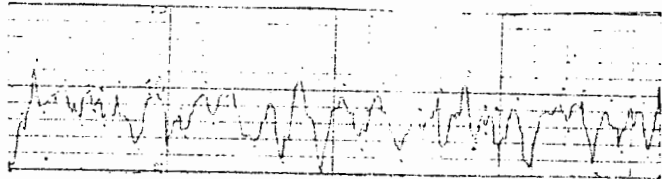
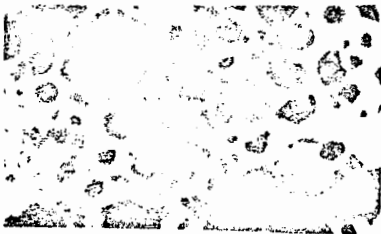


Exposure time 4 hrs

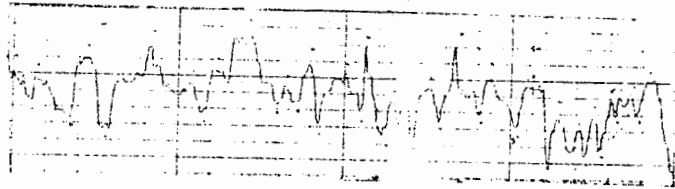
Fig 4 Photographs and profiles of typical damaged specimens at various exposure times,  $U=19$  m/s and  $\sigma=.06$ .



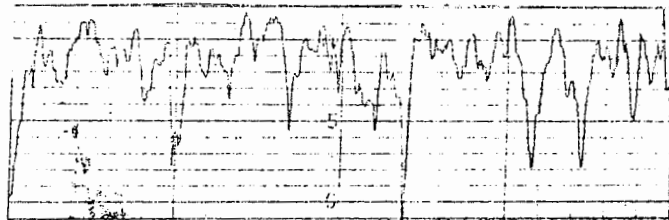
Exposure time 15 min.



Exposure time 35 min.

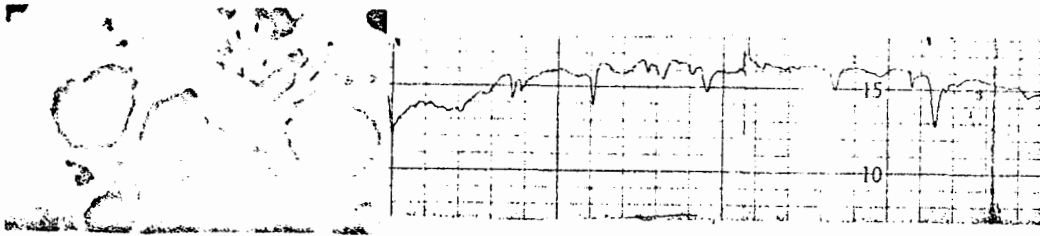


Exposure time 60 min.

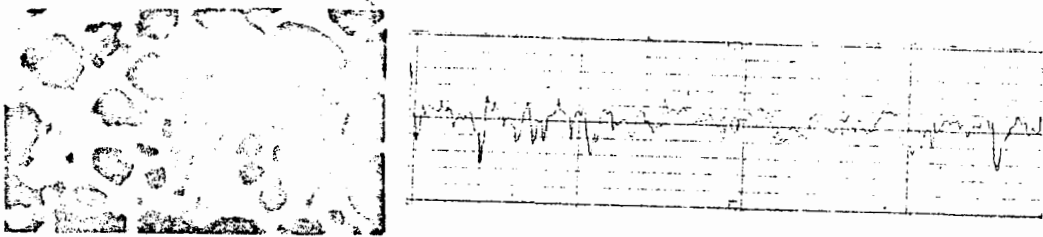


Exposure time 80 min.

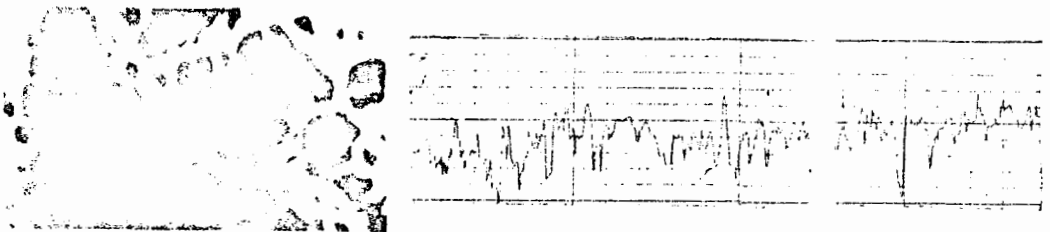
Fig 5 Photographs and profiles of typical damaged specimens at various exposure times,  $U = 26$  m/s and  $\sigma = .09$ .



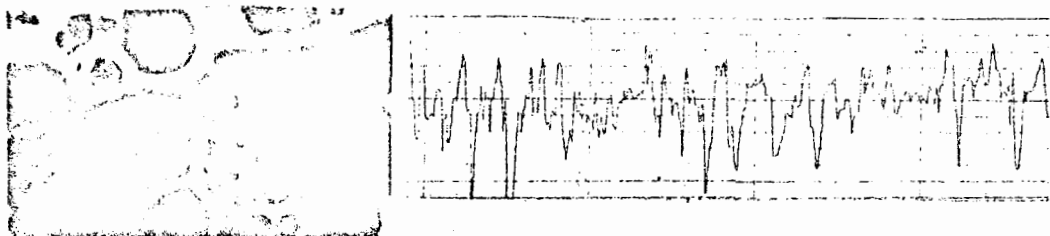
Exposure time 15 min.



Exposure time 30 min.



Exposure time 55 min.



Exposure time 75 min.

Fig 6 Photographs and profiles of typical damaged specimens at various exposure times,  $U=26$  m/s and  $\delta^*=0.025$ .

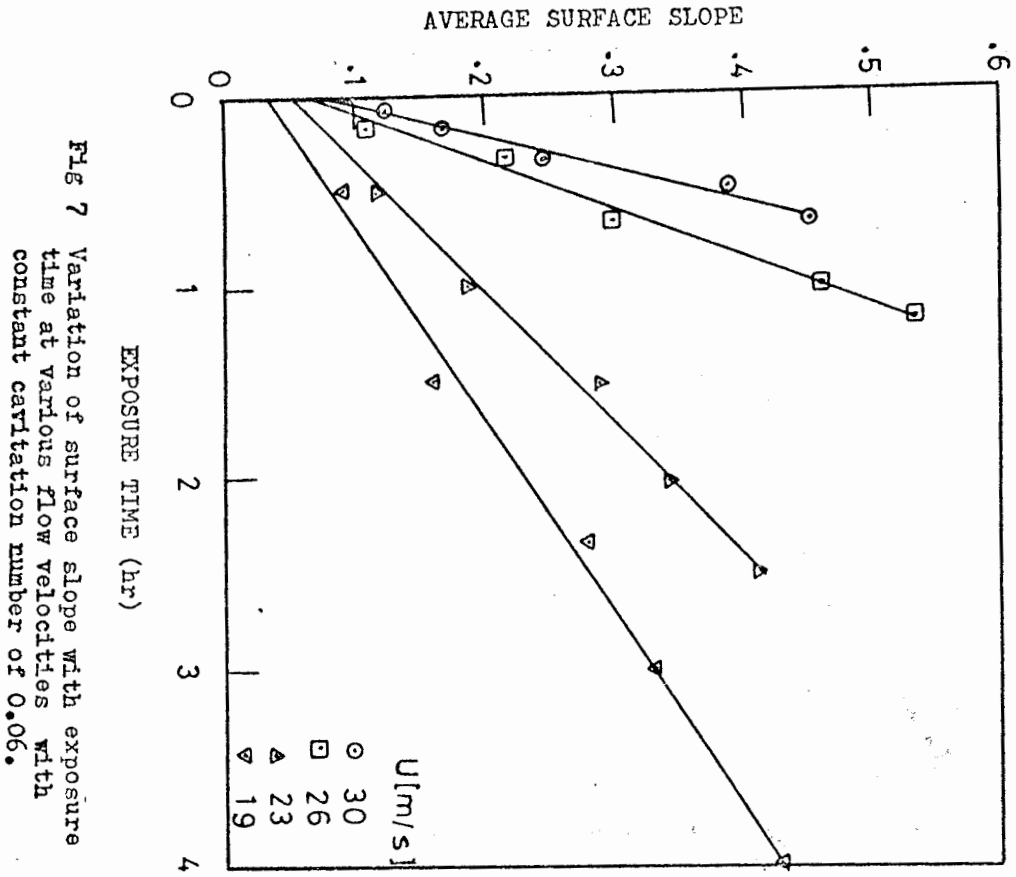


Fig 7 Variation of surface slope with exposure time at various flow velocities with constant cavitation number of 0.06.

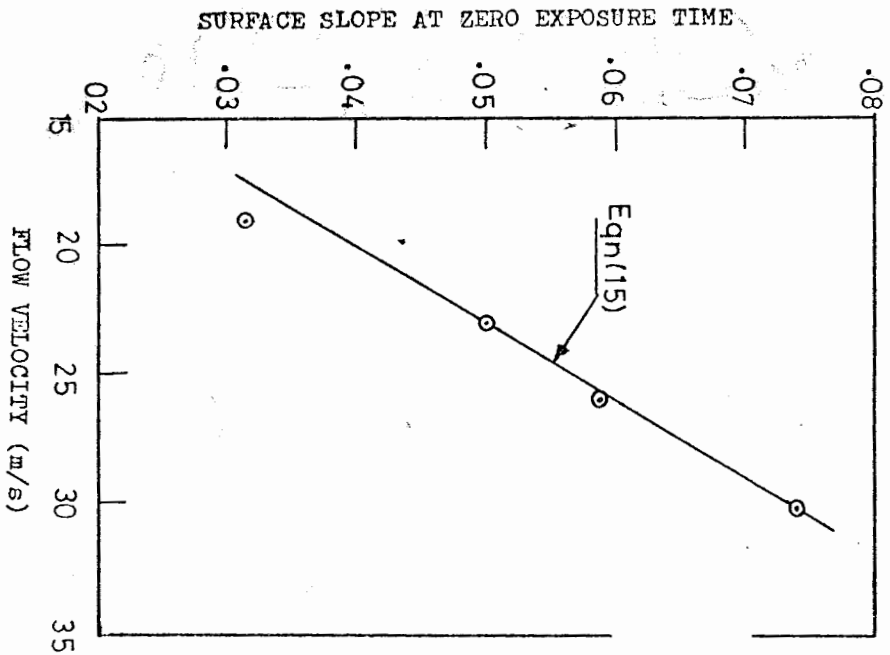


Fig 8 Comparison between measured surface slope with surface slope from equation (15) for tests at various velocities and  $\sigma = 0.06$

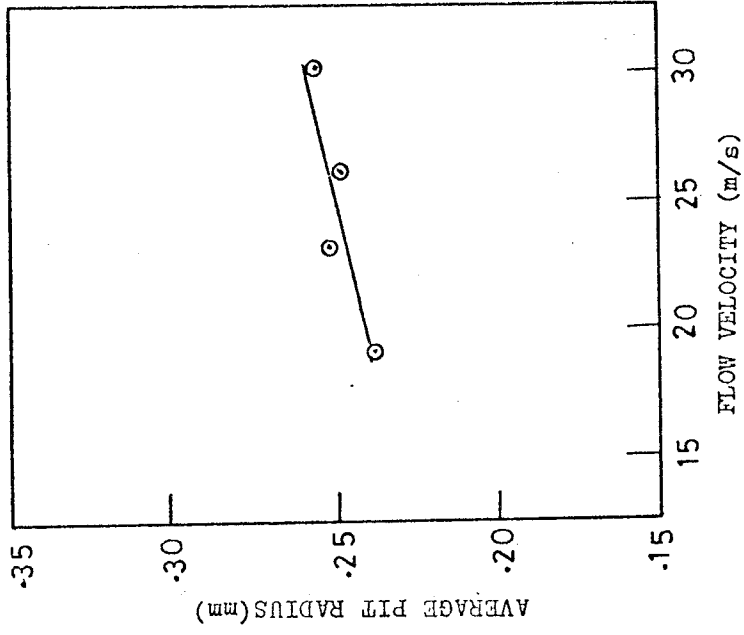


Fig 10 Mean pit radius as a function of flow velocity with  $\bar{v} = 0.06$ .

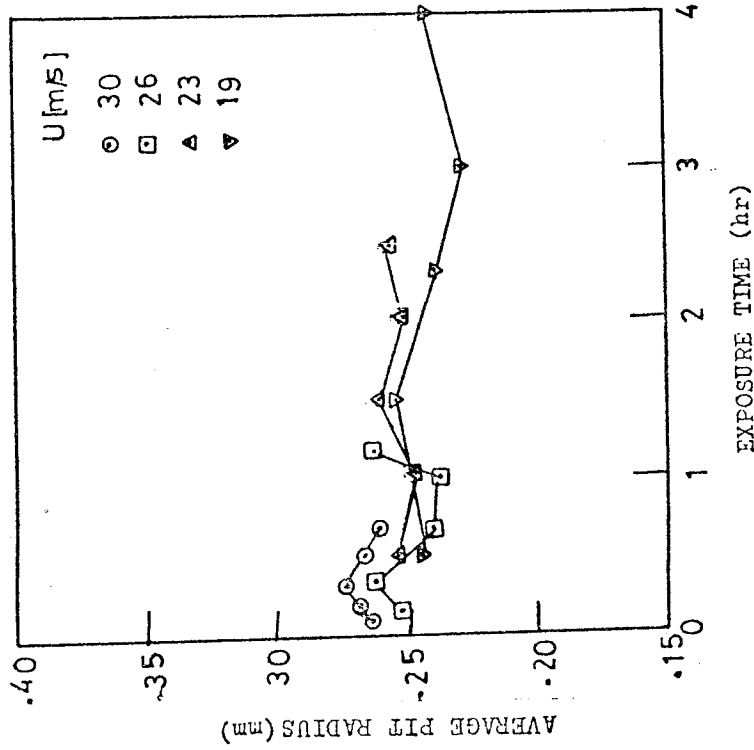


Fig 9 Variation of average pit radius with exposure time at different flow velocities and  $\bar{v} = 0.06$ .

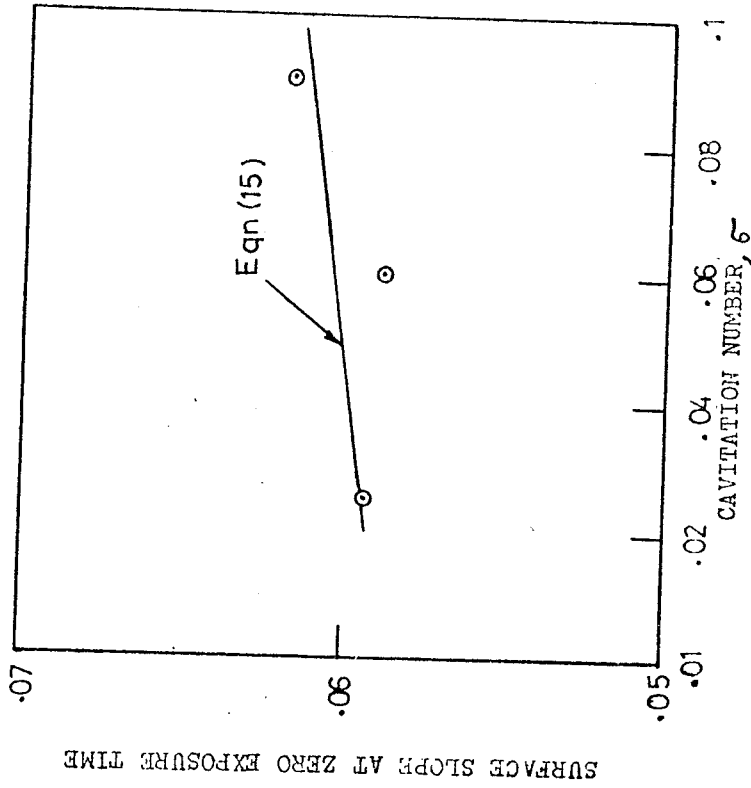


Fig 12 Comparison between measured surface slope with surface slope from equation(15) for tests at different cavitation numbers and  $U = 26$  m/s

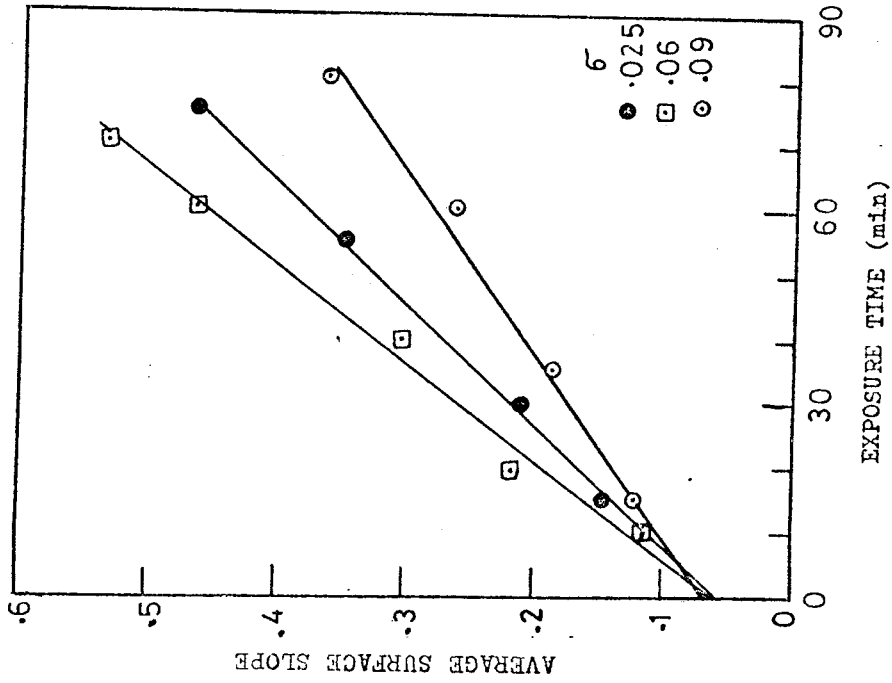


Fig 11 Surface slope vs exposure time at various cavitation numbers and  $U = 26$  m/s

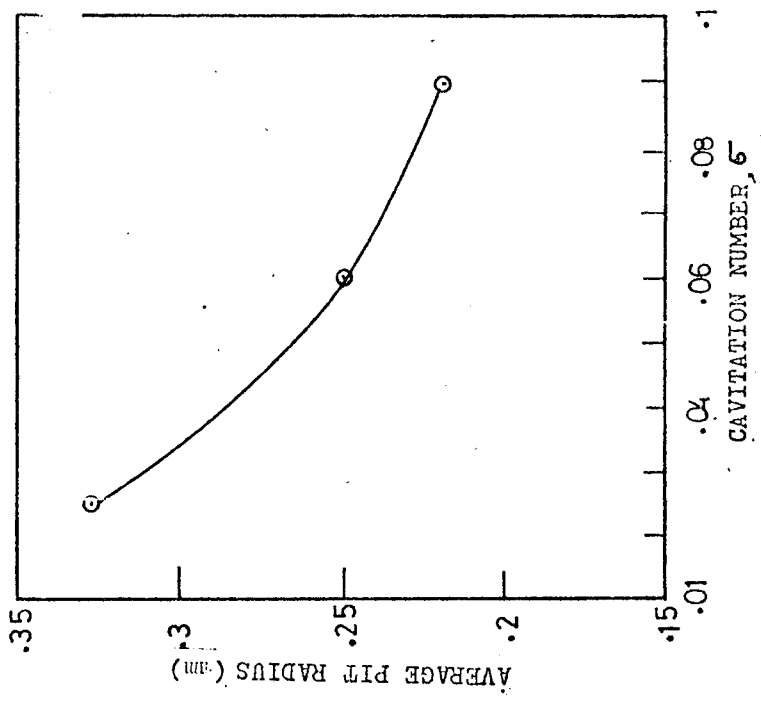


Fig 14 Average pit radius vs cavitation numbers at  $U = 26$  m/s

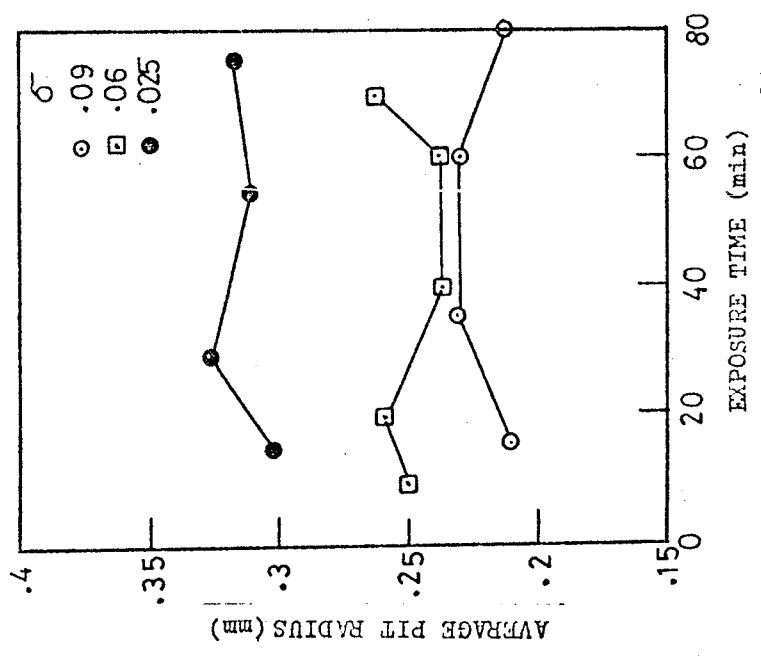


Fig 13 Average pit radius vs exposure time at  $U = 26$  m/s and various cavitation numbers ( $\sigma$ )